scientific reports

Check for updates

OPEN

Bioinspired surface structures for added shear stabilization in suction discs

Alyssa M. Hernandez[1,2,3]✉, Jessica A. Sandoval[1,2,3], Michelle C. Yuen[1,2] & Robert J. Wood[1,2]

Many aquatic organisms utilize suction-based organs to adhere to diverse substrates in unpredictable environments. For multiple fish species, these adhesive discs include a softer disc margin consisting of surface structures called papillae, which stabilize and seal on variable substrates. The size, arrangement, and density of these papillae are quite diverse among different species, generating complex disc patterns produced by these structures. Considering papillae arrangements in three fish species, the Northern Clingfish (*Gobiesox maeandricus*), Tidepool Snailfish (*Liparis florae*), and Chilean Clingfish (*Sicyases sanguineus*), we fabricated physical disc models that tested relevant surface pattern parameters under shear loading conditions. Parameters of interest included the area of papillae-like structures, the spacing between adjacent structures (channel spacing), and the percent coverage of elements relative to the total disc area. To create our models, a soft silicone elastomer was added to a stiff circular suction cup, which was then "stamped" using a laser-etched and thermoformed mold base to create the desired surface patterning. Discs were tested using a robotic arm equipped with a force sensor, which sheared them across smooth and rough surfaces at a fixed speed and distance. The arm was also used to vary the initial compression to test performance under both suction-dominant and friction-dominant preloads. For our designs, patterns with smaller papillae-like structures and channel spacing often produced higher peak forces than those with larger features. However, the design that withstood the highest shear load featured an intermediate pad size and channel spacing, potentially highlighting a balance between overall surface area and fluid channeling. Additionally, discs with surface patterns often outperformed the control discs (no pattern) on both smooth and rough surfaces, but performance was highly dependent on preload, with patterned discs exhibiting benefits with the higher "friction-dominant" preloads.

Keywords Adhesion, Biomimetics, Suction disc, Shear, Wet friction

There are numerous challenges for high strength, reversible, non-penetrative adhesion in marine environments. For example, wet/submerged substrates introduce a two-fold problem, as attachment devices must be able to conform to irregular surfaces[1] while mitigating a loss of friction caused by increased surface lubrication[2]. Additionally, aquatic environments often introduce forces (e.g., irregular or laminar flows), that threaten to dislodge attached objects. For underwater robotics, secure and reversible adhesion is critical for fields like conservation and exploration[3], which require reliable tools for monitoring (e.g., marine animal research[4,5]) or grasping (e.g., robotic manipulation[6,7]). To address such problems, researchers often take inspiration from organisms, some of which have specialized structures that help them adhere to various substrates in unpredictable environments. While these structures are diverse, many different groups of aquatic organisms (e.g., cephalopods, fish) utilize suction-based organs that help them perform a variety of tasks including as locomotion, feeding, or general attachment[8].

There are numerous examples of biological marine adhesion systems that have been used as inspiration for engineered adhesives. For example, octopus suckers represent a popular model system used to inspire successful and versatile underwater adhesion[9,10]. Various morphological features (e.g., sucker arrangement, stiffness) of this stable but reversible attachment system have been described[11], emphasizing the adaptability of the sucker-lined arms as they attach to and locomote across different surfaces as well as grasp potential prey[10]. Inspiration from these cephalopods have produced full robotic arms[12,13] as well as various singular sucker designs that can integrate sensors or actuation[14]. While these devices are useful for tasks such as robotic manipulation or

[1]John A. Paulson School of Engineering and Applied Sciences, Harvard University, Boston, MA 02134, USA. [2]Project CETI, New York, NY 10003, USA. [3]These authors contributed equally: Alyssa M. Hernandez and Jessica A. Sandoval. ✉email: ahernandez@g.harvard.edu

locomotion, other uses (for example, marine mammal monitoring) may require adhesive devices that remain stable under stronger shear forces. To counter such forces, researchers have studied the supporting structures (e.g., interlocking spines, hairs, surface texturing) of different biological suction discs, which enhance both friction and sealing in wet environments[15–17]. The species-specific diversity among these structures is notable, as slight morphological variations may indicate a response to certain environmental pressures. Therefore, understanding such variation would be informative for tailoring adhesive designs for specific tasks and substrates.

Morphological adaptations for shear-resistance in wet conditions have been described in the adhesive systems of many different organisms. For example, groups of disc-bearing fish have generated interest over the recent decade for their ability to strongly adhere onto a variety of substrates, such as rocky intertidal habitats[18,19] or marine mammal symbionts[20,21]. These fish often couple suction with various mechanisms of securement such as mechanical interlocking, soft sealing rims, or surface texturing for enhanced friction. For example, remoras secure themselves to various swimming hosts[21] via a suction disc that is supported by spinule-covered lamellae, which interlock with surface asperities[22]. Additionally, this disc has a soft lip that helps the disc remain sealed under shear loading[23]. Other fish groups such as riparian loaches resist strong river flows by using a whole body suction disc supported by frictional fin rays and sealing unculi[16,24]. Clingfish, lumpsuckers, and snailfish utilize soft papillae as a means to generate friction/sealing, but the size, arrangement, and abundance of these features is usually very different depending on the species[25,26]. As a result of these morphological studies, engineers have produced a variety of bioinspired designs that attempt to replicate the success of these diverse mechanisms of attachment[27–29].

While there have been many cases of species-specific studies for both biological organisms and bioinspired analogs, comparative studies remain somewhat limited. Because biomechanical testing with multiple species can be logistically challenging, some researchers have turned to physical models to compare structures of interest[22,30]. For our research, we were particularly interested in using models to explore the variation of disc papillae, as they represent a diverse surface structures that show up independently in multiple groups of aquatic organisms (e.g., remora[23], suckermouth catfish[17], and clingfish[28]). Previous studies of the surface papillae provides initial insight into their function in aquatic systems, highlighting their ability to deform on rougher surfaces to generate friction and strengthen sealing[26,31]. While there is a general consensus about potential papillae function, the diversity of their size, abundance, and arrangement (even among closely-related species), suggests adaptations for certain environmental conditions. For example, Krings et al.[17] produced a morphological study of the surface structures on the oral suction discs of several suckermouth catfish species. In addition to four different types of papillae, they also found texturing (eight types of unculi) on top of the structures. The species inhabited a diverse range of freshwater habitats with different flow rates and substrates for attachment. While no formal biomechanical testing was done, initial correlations between disc structures and habitat suggested particular morphological adaptations to stronger flows and rougher substrates (e.g., longer papillae in stronger flow environments for better interlocking)[17]. These functional morphology studies are informative, as they highlight parameters of interest (e.g., size, stiffness of the papillae) that can be explored through further biomechanical testing.

In this paper we utilized a unique silicone patterning technique to produce papillae-like structures on the interior surface of fabricated suction discs. This technique allowed us to generate multiple designs, producing a comparative study that evaluated parameters of interest for surface patterns. To evaluate relevant parameters that could be important to shear resistance, we took inspiration from the papillae arrangements of three fish species (Fig. 1a,b). For example, the Tidepool Snailfish (*Liparis florae*) has a small number of large papillae on the outside margin of its disc, with little variation in channel spacing between individual structures. Alternatively, the Northern Clingfish (*Gobiesox maeandricus*) has an abundance of much smaller papillae on the outside margin of its disc, with variations in spacing between the adjacent papillae. Finally, the Chilean Clingfish (*Sicyases sanguineus*) differs from the other two in that the papillae can be found throughout the disc (e.g., including within the chamber) instead of just along the outside margin.

To standardize these features of interest from our biological models, we tested three bioinspired surface parameters: the area of the individual papillae-like structures (Fig. 1c), the width of the channel spacing between individual structures (Fig. 1d), and the percent coverage of structures relative to the total disc area (Fig. 1e). While these parameters were varied, a standard hexagon shape was used for our papillae-like structures (referred to as "pads" throughout the rest of the paper), as this is a common wet adhesion pattern across many animal types (e.g., insects[32], frogs[33], newts[34], and fish[35]). Utilizing a robotic arm equipped with a force sensor, we tested adhesive performance of various designs under controlled shear loading. By highlighting this loading direction, we hope to mimic a biologically-relevant condition (e.g., shear forces induced by oncoming flow) that is important for suction disc research. We used this tool in previous work[36], which allowed us to control the speed and distance of the shear pull. In addition to shear loading, we wanted to explore how these rim structures would benefit discs with a variety of suction chamber depths (deep vs shallow discs). To accomplish this, the robotic arm controlled the initial normal preload of the discs before the shear pull. Varying this parameter produced suction-dominated (small preload) and friction-dominated (large preload) states that evaluated the balance between surface contact and suction.

For this study, we first tested our patterned designs on a smooth surface under a more suction-dominant preload. We hypothesized there would not be huge variations in performance on this "ideal" surface, as a smaller portion of the disc's interior surface would be making contact with the substrate. Therefore any strong seal would assist with shear forces. However, these results would inform our follow up experiments using higher preloads (friction-dominant). We anticipated that a friction-dominant preload would show the true benefit of the different patterns as this would produce more contact of the papillae-like pads as well as channel area for removal of excess water. Additionally, further testing on rougher surfaces would highlight another benefit of patterned discs, because these rim structures might deform when contacting asperities, enhancing adhesive performance. Overall, our study was designed to better understand parameters for shear resistance in adhesive

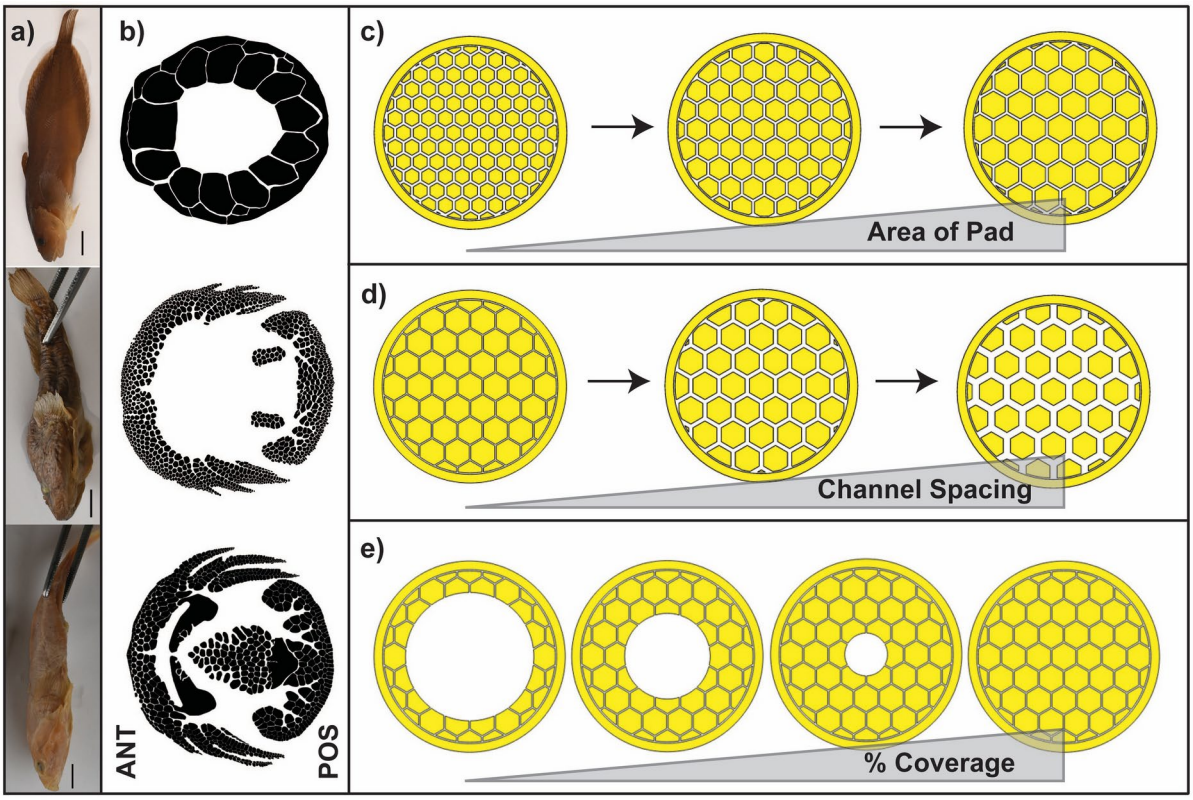

Figure 1. Inspiration from adhesive fish to the design parameters for patterned suction discs. (**a**) Side profiles of the representative fish species: Tidepool Snailfish (*Liparis florae*; top), Northern Clingfish (*Gobiesox maeandricus*; middle), and the Chilean Clingfish (*Sicyases sanguineus*; bottom). Scale bar = 1 cm. Specimens used for photos were provided by Museum of Comparative Zoology, Harvard University, Photo credit: Michelle Yuen. (**b**) Binary image representations of the the papillae on their adhesive discs. Image credit: Jessica Sandoval. Anterior (ANT) and posterior (POS) labels highlight the orientation on the disc in relation to the head and tail of the fish. The variations in the papillae arrangements of these fish inspired the investigation of the following design parameters: (**c**) Surface area of the pad features (A_{pad}, ranging from 10 to 50 mm^2); (**d**) channel spacing (ranging from 0.3 to 1.9 mm); and (**e**) percent coverage of the suction disc (25–100%). Papillae-like structures will be referred to as "pads" throughout this paper.

discs, and we sought to 1) produce a comparative study that explores multiple parameters of interest for disc surface structures, 2) develop a new methodology for applying patterns to non-planar suction disc geometries, and 3) understand how to tailor bioinspired suction discs for lateral flow regimes by coupling rim surface features with the initial state of the disc (e.g., deep vs shallow suction chamber). By exploring these disc properties, we not only hope to improve designs for biomimetic adhesives, but also highlight how engineering-based methods can produce appropriate models for comparative biological studies.

Results

Shear performance of patterned suction discs under suction-dominant conditions

Using the robotic arm setup, we tested how certain surface pattern parameters (pad area, channel width, and percent coverage) impacted shear performance (maximum shear load) on smooth and rough wetted surfaces. In addition to these parameters, the amount of compression applied to the discs, prior to shearing, was varied to test how initial preload affects performance. For all experiments, the suction discs were mounted rigidly to the end of a robotic arm which was equipped with a six degree-of-freedom force-torque sensor. The disc was pressed down onto the surface to 10 N to fully engage the disc, then pulled up to release the compressive load to a preload value ranging from 2 N to 10 N, and then translated across the surface for a fixed distance while the shear force was recorded. Smaller preloads (e.g., 2 N) produced a larger chamber within the disc resulting in a "suction-dominant" preload. Larger preloads (e.g., 10 N) would press the disc into the surface, producing more contact between the rim and the substrate, which resulted in "friction-dominant" adhesion behavior. In the suction-dominant case, a suction chamber provides adhesion via the pressure differential between the ambient and chamber interior; in the friction-dominant case, the shearing motion is resisted by the frictional forces between the suction disc interior and the surface.

We first investigated the effect of pad area and channel width of discs in a "suction-dominant" condition (2 N preload) on a smooth, wet surface. Before testing our patterned discs, we tested a control disc (uniform soft rim with no pattern) to generate a baseline for comparison. For our patterned designs, the labels used in the text for

Pad area		Channel width	
A10	10 mm^2	C1	0.32 mm
A15	15 mm^2	C2	0.65 mm
A20	20 mm^2	C3	1.14 mm
A30	30 mm^2	C4	1.57 mm
A40	40 mm^2	C5	1.89 mm
A50	50 mm^2	–	–

Table 1. Table showing pad areas and channel widths as measured after thermoforming into their 3D geometries. The channels all had a final depth of 300 μm.

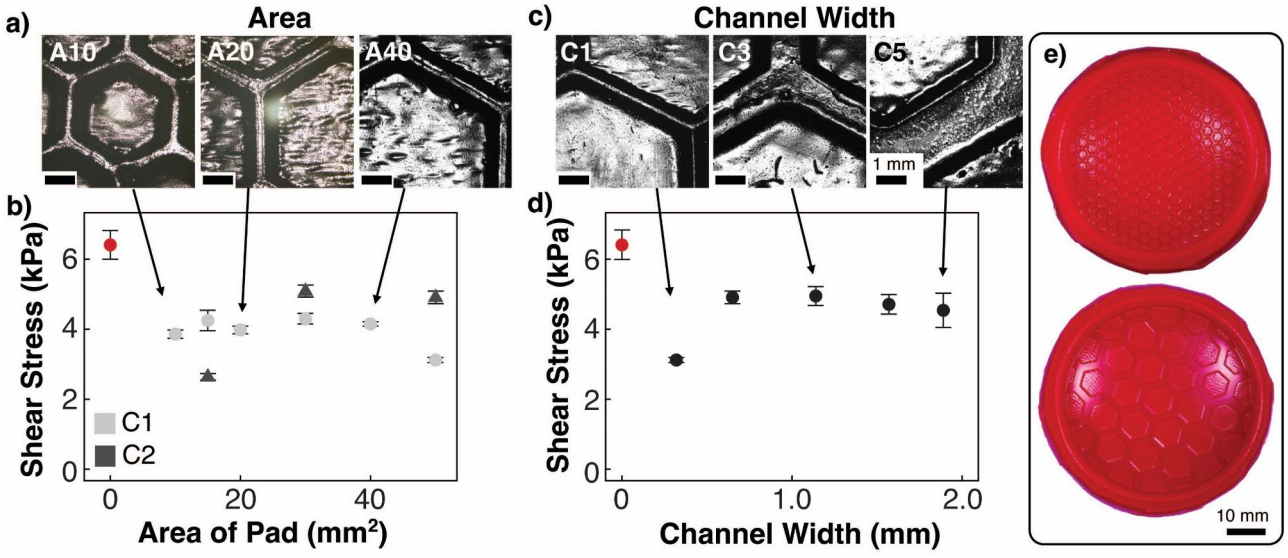

Figure 2. Investigating surface parameters (pad area and channel width) under a suction-dominant preload (2 N). (**a**) Micrographs of the molds used to generate the areas of A10 (8.7 ± 1.1 mm^2), A20 (20.9 ± 0.9 mm^2), and A40 (39.0 ± 2.7 mm^2), all with a channel width of 0.65 mm (C2). Scale bar, 1 mm. (**b**) Effect of changing the surface area of the pad on the resulting shear stress (kPa) for a suction disc preloaded to the surface by 2 N. Light grey dots (mean) and error bars (S.D.) represent designs with a set channel width of 0.32 mm (C1). Dark grey triangles (mean) and error bars (S.D.) represent designs with a set channel width of 0.65 mm (C2). The red circle represents the control disc. All samples were run in triplicate. (**c**) Micrographs of the molds used to generate different channel widths—a narrow (0.32 mm, C1), an intermediate (1.14 mm, C3), and a wide channel (1.89 mm, C5). Scale bar, 1 mm. (**d**) Effect of the channel width (mm) on the resulting shear stress (kPa) for a suction disc preloaded to a surface by 2 N. Black dots and error bars (mean±S.D.) represent designs with a set pad area of 50 mm^2 (A50). The red circle represents the control disc. All samples were run in triplicate. (**e**) Images of the patterns of the suction discs. The smallest pad size and narrowest channel width (A10, C1; top) and the largest pad size and widest channels (A50, C5; bottom). Scale bar 10 mm.

pad area and channel width and their corresponding measured values are listed in Table 1. We first varied pad area at fixed channel width (Fig. 2a,b). We observed that for the smaller channel width (C1, light grey markers in Fig. 2b), increasing the area of the pad (A10–A40) did not greatly affect the maximum shear stress that the disc was able to withstand, until the largest pad area (A50) where performance degraded by about 25%. With wider channels (C2, dark grey markers), however, we observed that the shear performance of larger area pads improved. To study this effect further, we tested discs with the largest pad area (A50) across a range of channel widths (C1–C5) (Fig. 2c,d). Further increasing the channel width did not appear to improve performance further, and subsequent tests examined the effect of the two smallest channel widths. From these experiments, there appear to be a combined effect between the pad area and channel width on the discs' shear performance. Additionally, all designs had lower performance than the control disc. Since these experiments were conducted in the suction-dominant configuration, only part of the disc interior was in contact with the surface. Because the contact of the rim was lower and suction was the dominating factor in adhesion, we suspected the impact of the pads/channels were not apparent on the smooth surface in this configuration. Therefore, follow-up experiments focused on a larger preload and rougher substrates.

Shear performance of patterned suction discs under friction-dominant conditions

To further investigate the effect of the surface structures on shear performance, we tested the discs in a pure-friction condition where the discs were pushed fully onto the surface and held in the fully-compressed position (10 N preload) while being sheared across the surface. Under these conditions, we compared the shear performance of discs with a combination of pad areas (A15, A30, A50) and channel widths (C1, C2), as well as with a smooth, unpatterned disc as the control case. We found that there was indeed a confounding effect between the pad area and channel width, as seen in Fig. 3. The narrower channel (C1) paired with a smaller pad area yielded a higher peak shear stress. When the channel width was increased (C2), the medium pad area (A30) discs showed increased performance, whereas the performance of discs with the smallest pad areas suffered. Also, the performance of the smooth control disc showed a large dropoff in performance compared to the previous 2 N preload tests. In additional experiments, the amount of preload was used to indirectly alter the amount of patterned area in contact with the surface. In order to independently ascertain the effect of coverage fraction of the patterned surface, we systematically molded the structures from the outer perimeter, radiating inwards (Fig. 3b,c). We found that as the amount of structures covering the interior of the disc increased, the shear stress that the disc could withstand also increased, with the sharpest increase occurring between no structures and 25% coverage.

Shear performance under variable preload on smooth and rough surfaces

When deployed, the suction discs will experience a range of preload values across the suction- and friction-dominant modes (Fig. 4A). To investigate disc performance as preload is varied, we subjected the best performing patterned suction disc (A30, C2) and a smooth control disc to a range of preload values from 2 to 10 N on a smooth surface (Fig. 4B) and a microrough (Fig. 4C) sandpaper surface. On smooth surfaces, the control disc outperformed the bioinspired patterned disc at low preloads, which reflects the better sealed suction chamber in the control disc. However, at higher preloads, the bioinspired disc outperformed the control disc. The variable preload experiments were also conducted on a rigid, microrough surface with feature sizes on the order of 40.5μ m (P360 sandpaper). In addition to the patterned and control discs, we additionally tested the performance of a smooth disc without the soft silicone layer. On the microrough surface, the discs are less effective at forming a seal against the surface to create a persistent suction chamber. As a result, shear values decreased, particularly for the control disc. As the preload increased, increasing the contact area between the disc and the surface, the performance of the patterned disc improved, while the control disc's performance deteriorated.

Shear performance under friction-dominant conditions on different rough surfaces

Building off the these preload tests, we evaluated the three disc designs (bioinspired, control soft rim, and control stiff) on two additional rough surfaces (Fig. 4d). We refer to these sandpaper surfaces as medium rough (grain size: 68 μm) and rough (grain size: 201 μm). Performance on a medium rough surface was similar to our microrough surface, with the bioinspired disc outperforming both control discs (with and without the soft rim). However, unlike the microrough surface, it only slightly outperformed the control disc with the soft rim. Additionally, the control disc with the soft rim outperformed the stiff control disc, which it had not done on the microrough surface. On the roughest surface, there was a slight drop-off in the performance of the bioinspired disc. Interestingly, the performance of the control disc with the soft rim increased on this surface compared to the medium grit surface, and slightly outperformed the bioinspired disc.

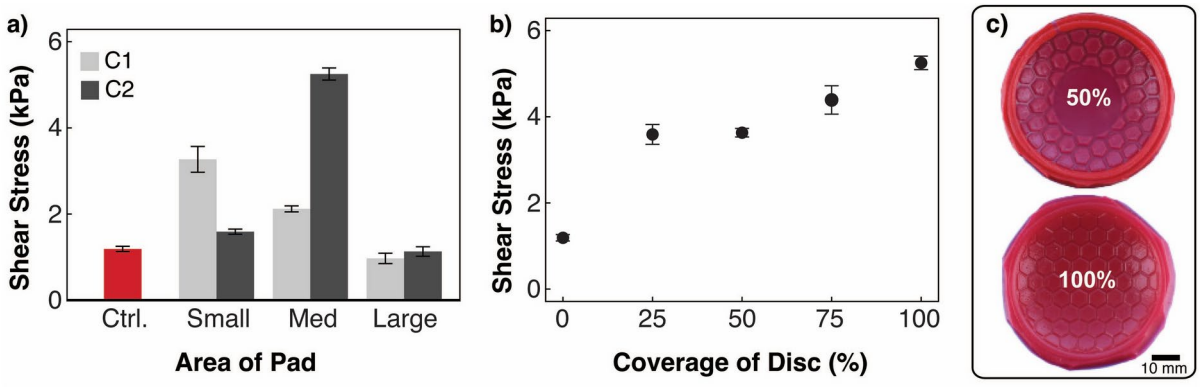

Figure 3. Investigating surface parameters (pad area, channel width, coverage) under a friction-dominant preload (10 N). (**a**) Measuring the trade-off of area and channel width on the resulting shear force (kPa). The patterns tested were either small (A15), medium (A30), or large (A50), and with a channel width that was either 0.32 mm (C1; light grey) or 0.65 mm (C2; dark grey), or a control (red). Preload, 10 N. (**b**) The effect of percent coverage of disc pattern on the shear stress (kPa). In addition to a control disc (0%), we tested coverage variations (25%, 50%, 75%, and 100%) of our best-performing disc (A30, C2) from the previous experiments. Preload, 10 N. All samples for a and b were run in triplicate. (**c**). Images of patterned suction discs (A30, C2) with 50% (top) and 100% (bottom) coverage.

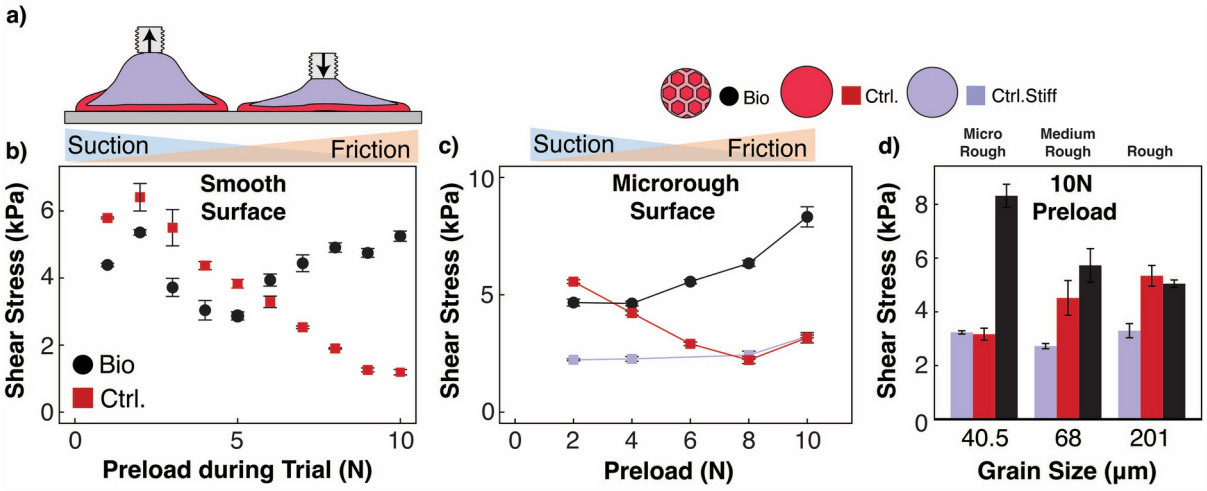

Figure 4. Shear performance of control discs and best-performing disc (A30, C2) under variable preloads on smooth and rough surfaces. (**a**) Schematic of the suction discs while subjected to different preloads. The discs were first pressed to the surface by a preload of 10 N, and either retracted vertically to ease the load to 2 N (left) or maintained a full, compressive preload of 10 N (right). (**b**) We varied the preload of our best-performing, bioinspired suction disc (A30, C2; black circles) and a control disc (no structures; red squares). All discs were engaged with a smooth surface by a preload of 10 N and retracted vertically until reaching a final preload prior to starting the trial. Lower resulting preloads implied a greater role of suction, whereas higher preloads involved a greater role of friction. (**c**) Effect of a microrough surface on the shear stress (kPa) of different suction discs across different preloads (N). (**d**) Effect of different rough surfaces on the shear stress (kPa) of different suction discs under a 10 N preload. For plots (**c**) and (**d**), we tested a bioinspired, patterned suction disc (A30, C2; black), a control suction disc with a smooth, elastomeric layer (red), and a control suction disc without a smooth elastomeric layer (purple). All samples for b, c, and d were run in triplicate.

Discussion

The balance between surface structures and fluid channeling

For our first two parameters of interest (pad area and channel spacing), we anticipated that there would be trade-offs for different design combinations. For example, having narrower channels would increase the total frictional area available for larger papillae-like pads, but excess water could be retained between the disc and the substrate due to minimized channel volume. Such excess water would lead to hydroplaning and loss of surface contact.

To further understand this relationship, we calculated the amount of surface area lost by increasing the channel size by ≈6×, from C1 (0.32 mm) to C5 (1.89 mm) for A50 (50 mm^2). This increase resulted in a roughly 30% reduction in the total surface area of the pads across the entire suction disc. However, the widest channels, and thus lowest total surface area, resulted in a ≈1.5× higher shear stress than the narrowest channels (A50, 2 N preload; Fig. 2d). This finding suggests that, despite resulting in the highest total surface area, the narrowest channels (C1) were not sufficient in shuttling fluid away from the surface and corresponded with the lowest shear stress values for that trial. Balancing channel width and individual pad area are crucial to optimizing suction discs for fluid channeling and frictional interactions, both of which are key for withstanding shear loads.

This intricacy was especially apparent for the smaller (A15) and larger (A50) pads (2 N preload; Fig. 2), as small pads performed better with smaller channels (C1) and larger pads performed better with larger channels (C2). For the smaller pads, having too much area dedicated to the channels may reduce the pad area available for frictional interactions. Alternatively for the large pads, more area is allocated for these frictional elements, so having narrower channels most likely traps some water underneath the rim leading to hydroplaning. Interestingly, our medium pad area (A30) demonstrated high shear stress across both channel widths, which may highlight an "intermediate" pad size suitable for shear resistance.

In addition to our designs, we concluded that performance was highly dependent on the type of preload. We tested two preload types: suction-dominant (2 N) and friction-dominant (10 N). Under suction-dominant preload, the disc was pulled from the surface to a load of 2 N, which increased the volume of the suction chamber and reduced the footprint of the disc. A smaller fraction of the rim, and thus a smaller fraction of the pads, was in contact with the substrate. In a friction-dominant preload, the disc was pushed to the surface and maintained under a 10 N compressive load. This compressive preload considerably reduced the volume of the suction chamber and increased the total quantity of pads engaged with the surface.

In first evaluating the relationship between channel size and pad area based on preloads, we observed differences between the effect of 10 N and 2 N preloads (Fig. 3a). Under a friction-dominant 10 N preload, the performance of the control exhibited 75% less shear stress compared to the 2 N preload (suction-dominant). Additionally, we observed heightened differences based on preload in the effect of channel spacing, most notably in the "Medium" pad area (A30) suction disc. In a friction-dominant preload, intermediate pad sizes coupled with wider channels resulted in a 2.5× higher shear stress, as compared to narrower channels (C2 vs C1, A30,

10 N preload). This difference was more pronounced than in the suction-dominant trial as a greater amount of the suction disc was engaged with the surface under higher compressive preloads. The difference between the control and the top-performing, medium-area, wider-channel disc (A30, C2) under high compressive preloads demonstrates the need for fluid channeling to prevent hydroplaning and improve shear stress performance.

Previous work describing channel networks in the adhesive pads of different organisms often note how these channels are useful in removing excess fluid from wet contact surfaces[35,37]. For example, the adhesive performance of the toe pads in various groups of frogs (e.g., tree and torrent frogs) has been evaluated under wet conditions, highlighting the morphology of the epithelial cells (which serve a similar purpose to papillae) and the surrounding fluid channels[38]. The morphology of the cells can be quite variable, with groups like torrent frogs having more elongated cells. It has been suggested that this particular shape is beneficial in faster flow environments, as the elongated cells produce "straighter, shorter channels"[39]. As our discs are tested in shear, smaller to intermediate pads sizes may receive some benefit from the shorter channel length. Throughout our various experiments, we found one best performing disc (A30, C2), which had a pad size of $30\ \mathrm{mm}^2$ and channel size of 0.7 mm. This potentially reflects certain trade-offs that help balance inherent trade-offs: the "medium" pad size has enough area to generate friction, but is not too large to limit the volume of the channels.

More surface structures are beneficial for higher disc preloads

For the percent coverage of the papillae-like pads, we found that 100% coverage of the disc resulted in the highest shear stress, when compared to lower percent coverages. We coupled this result with FTIR images of the 100% coverage suction disc (Fig. S2) while preloading it to a surface and subjecting it to shear loads. Engaging a suction disc to a surface resulted in the formation of a suction chamber that was not in contact with a substrate. However, when subjected to shear loads, the area in contact shifted, spreading the contact to the pads within the inner suction chamber, which were previously not engaged with the substrate. This observation supported the finding that more coverage corresponded with greater shear stresses.

We also found that surface structures are most advantageous when the disc is more compressed (10 N preload) to the surface (Fig. 3b). As expected, the higher preload generates the most disc contact such that more protruding features can engage with the substrate. In biology, disc coverage is an important parameter to consider, as certain species of clingfish have a higher proportion of papillae throughout their disc[25]. For example, our biological inspiration for disc coverage, the Chilean clingfish (*Sicyases sanguineus*), is a large species of clingfish found exclusively on the Pacific coast of South America[40]. Its large adhesive disc hosts numerous papillae, with a cluster of large, flat papillae at the center of its disc[25]. It has been suggested that this large proportion of papillae is a result of the fish's size and unique ecology, as it is often found hanging on exposed, vertical rock walls well above intertidal waters[40].

Interestingly, these higher proportions of papillae can also be found in the discs of smaller clingfish species, which highlights a potential need based on certain environmental conditions (e.g., surface or flow rate)[25,41]. For example, smaller clingfish within the genus *Discotrema* are symbionts of reef-protected crinoids (sea lilies), and can often be found among the organism's feathery arms[42]. The discs of these clingfish host different sizes of papillae on the margin in addition to various clusters of small papillae throughout the ventral surface of the interior[41,42]. This abundance of surface structures throughout the disc could aid in secure attachment to the rougher, curved surfaces of the crinoid arms which also move with the flow of the water. Additionally, some of the larger papillae on the interior margin have a stiff keratinized "cap", which is a feature not described in other clingfish groups[41]. The presence of these features may highlight a unique adaptation that provides some kind of additional friction/interlocking needed for attachment.

Tailoring suction discs for the load type and surface

While we were able to determine a high-performing design (A30, C2) for our tests using two different preloads (2 N and 10 N), we incorporated this design into additional preload tests, which evaluated the trade-offs between suction and contact (Fig. 4). This included expanding our range of preloads to include increments between 1 and 10 N, testing three designs on a smooth and rough surface. On our smooth surface, the shear performance of our control disc (no channels) peaked at a preload of 2 N and gradually degraded over time (Fig. 4b). Our best-performing bioinspired disc showed a similar pattern up until about 5 N and forces gradually increased again from 5 to 10 N preloads. As preload increases, the volume of the chamber likely decreases, reducing the impact of suction. While this degrades the performance of both discs from 2–5 N preloads, the bioinspired disc recovers as more of the soft pad structures come into contact with the surface. As the presence of channels was the only difference between the two designs, we concluded that they must be redistributing the water underneath the rim.

The interplay between suction and friction becomes more complex on rougher surfaces (Fig. 4c,d). In this case, our control disc once again saw shear performance degrade from a 2-8 N preload. However unlike the smooth surface, there was a slight increase in force at the highest preload (10 N). The performance of the bioinspired disc was markedly improved on the microrough surface, as the preload increased, the shear stress increased and was considered top-performing. These forces often exceeded shear adhesion we observed on the smooth surface. This jump in performance for the bioinspired disc is most likely a combination of two parameters: fluid channeling and potential deformation of the pad conforming to the asperities of the microrough surface.

We evaluated the effect of the channels on a range of surface roughnesses in a friction-dominant preload. The bioinspired disc with channels outperformed all other discs on micro to medium roughnesses, achieving up to $\approx 2.5\times$ higher shear stress in comparison to the control. The channels could have aided in the shear stress by shuttling fluid away from the interface to improve surface contact, reducing the effect of hydroplaning[43]. Additionally, with this increased contact, the individual pads may have also deformed to better conform with the surface asperities.

As the grain size increased, the control with its continuous soft disc margin improved in performance, eventually overtaking the bioinspired disc on the roughest surface. Because this disc did not have the benefit of the channels, we concluded that it would retain the water left underneath its surface, as seen in its poor adhesion on the smooth surface. However, on a rougher surface, this water could be shuttled into the valleys in between the asperities[43]. On the microrough surface, the performance of the control disc was still poor, most likely a result of small height of the asperities (Fig. 4d). However, as asperity size increased, water was shuttled into deeper valleys, and the larger asperities were able to make better contact with the smooth disc margin[43]. Alternatively, the largest asperities may be detrimental to the bioinspired disc, as the grain size may have blocked fluid channeling, reducing performance.

Previous investigations into fish adhesion often describes how these papillae could potentially deform to to aid in sealing[17,31]. However, less work has evaluated the effect of preload in the presence of channels. Chamber depth is most likely an important parameter when it comes to performance of adhesive discs in fish species, and these preload tests provide some initial insight into how these dynamics might correlate to papillae diversity. Also, this insight into preload for different surface roughnesses is important for how these designs could be utilized in the field. Substrates within the field feature a wide array of surface roughnesses onto which attachment is critical. To achieve sustained adhesion, discs would need to be tailored for the substrate roughness and expected loads (e.g., wildlife monitoring tags). Tasks that utilize temporary adhesion (e.g., locomotion or manipulation) would also need to evaluate how the discs are being loaded onto surfaces, as ease of detachment would be an important consideration.

Future work

The diversity of surface structures in adhesive discs provides an abundance of avenues for future research studies. As we aim to improve the performance of bioinspired discs, it is important to evaluate relevant characteristics from their biological counterparts. For example, while our current designs had some light texturing on the surfaces of the papillae-like pads due to the initial rastering of the mold, this "microroughness" was consistent throughout all discs. Using our stamping method, certain patterns can be intentionally rastered upon the papillae-inspired sections of the molds, mimicking the unculi-like structures seen in several biological discs[16,17]. This smaller-scale texturing would be beneficial to understand as we try to increase friction for rougher substrates. In addition to this papillae microstructuring, multi-material molding processes could produce papillae-like structures with variable stiffness gradients, highlighting another biological parameter that could be evaluated with experimental work[17,41].

While adding microstructuring on top of larger-scale features might enhance the frictional properties of our discs, there are additional avenues for future research that could improve the performance of our papillae-like structures. For example, these structures can be broken down even further into smaller areas, highlighting the idea of contact splitting, which is a common adaptation in the adhesive foot pads of geckos and various insects[44]. These fibrillar structures enhance adhesion by using numerous nano and micro scale contacts to conform to substrates.[45,46]. These fibrillar adhesive systems are especially effective on rougher surfaces, as these contacts are often able to fit in between asperities, and the compliance of the individual hairs makes them more resistant to damage compared to a larger, conformable pad[45]. In terms of fish, some species of clingish (e.g. the Northern Clingfish) have an abundance of small papillae, which may reflect an adaptation to rocky substrates in intertidal zones. Testing patterns that reflect these numerous smaller features on substrates that are not only rough, but variable in curvature and compliance, would be a worthwhile exploration.

Additionally, while our work tested multiple disc preloads, our shear pull was set to a single speed and distance, mimicking a slow laminar flow. To evaluate adhesive performance across more diverse conditions, future experiments should integrate other ecologically-relevant parameters including flow speed. For example, the speed of the shear pull can be increased to better evaluate adhesion under stronger laminar or turbulent forces (e.g., riparian environments, swimming hosts). Our robotic arm setup can also be used to command motion along multiple directions, imitating more unpredictable conditions such as intertidal zones, which often host an abundance of disc-bearing organisms.

Methods

Design parameters

The suction discs of adhesive fish display a multitude of different pattern types. Using an image-stitching and binary conversion technique reported in previous work[35], we took three representative fish as inspiration for this study—the Northern Clingfish (*Gobiesox maeandricus*), Tidepool Snailfish (*Liparis florae*), and the Chilean Clingfish (*Sicyases sanguineus*). A visual comparison of these biological patterns brings about three predominant differences—the size of the individual pattern elements, the spacing between individual pattern elements, and the overall percentage of the suction disc that is covered in the pattern. In this work, we generated synthetic suction discs that varied in either the surface area of each individual hexagonal pad (A_{Pad}), the channel spacing between pattern elements (C), and the overall percent coverage of the internal surface area of the suction chamber (Fig. 5c).

Fabrication of suction discs

The suction disc and its corresponding three-part mold were modeled using computer aided design (Fusion 360, Autodesk, Inc.). The suction disc featured a circular footprint (diameter, 60 mm; aspect ratio, 1), wall thickness of 3 mm, chamber depth of 8 mm, and a stem (14 mm, height; 8 mm diam). The three-part mold was fabricated using two different fabrication processes. The body of the mold for the suction disc was fabricated with polylactic acid filament (Prusament, Prusa Research, Inc.) using a 3D printer (i3 MK3S, Prusa Research, Inc.). The bottom

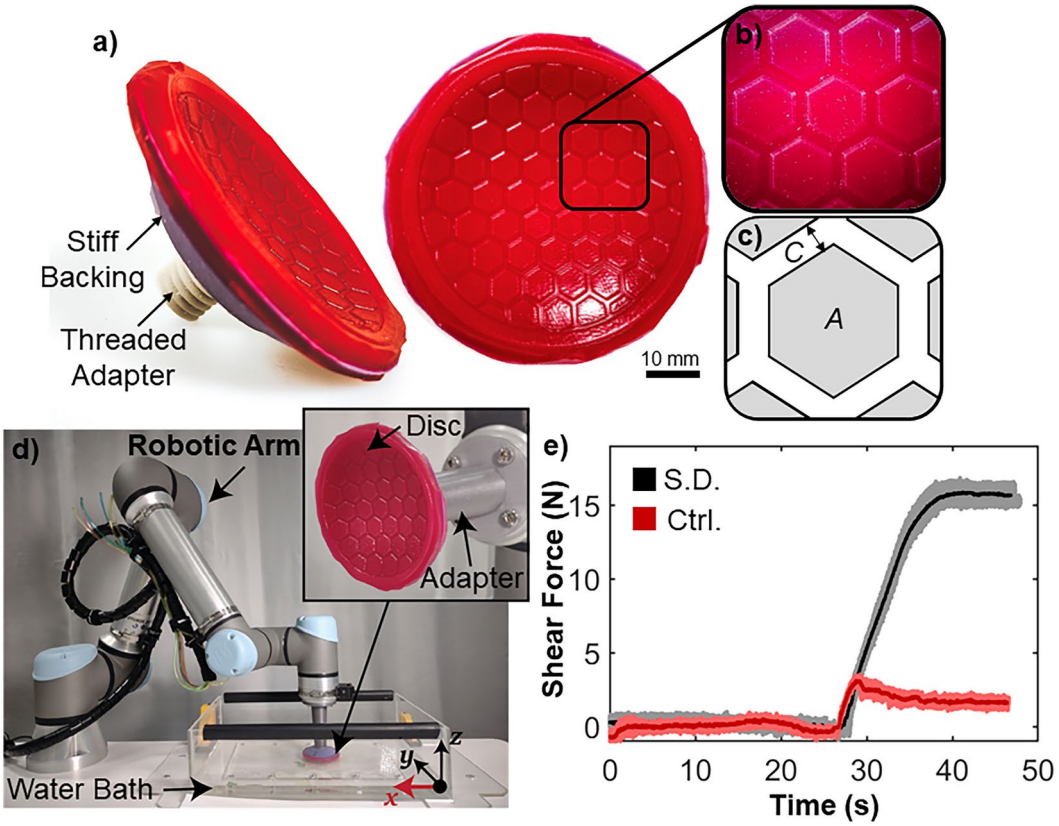

Figure 5. Mechanical testing setup of the adhesive discs using a robotic arm. (**a**) The fish-inspired suction discs features a stiff silicone backing and a pattern of regular hexagons across the bottom of the disc. A threaded adapter interfaces the disc with a robotic arm. Scale bar, 10 mm. (**b**) A pattern of regular hexagons (A30, C2) . (**c**) Parameters varied across the trials include the channel width (*C*) and the area of the individual pads (*A*). (**d**) A patterned suction disc (inset) is secured to an adapter and attached to the end effector of a robotic arm. Trials occurred in a waterbath along a smooth acrylic or rough sandpaper surface (for sandpaper profiles, see Fig. S1). Shear tests were performed along the *x*-direction. (**e**) Example data curve of shear force (N) and time (s) from the robotic arm during trials. A suction disc (A30, C2; black) was compared to the control (no patterning; red). Each trial was performed in triplicate and averaged across the trials.

of the mold was fabricated using photocurable resin (Vero White, Stratasys, Inc.) in a 3D printer (Objet350 Connex3, Stratasys, Inc.) to form a smooth, non-porous base.

Suction discs were molded in a process similar to previous studies[28,36]. To cast the main body of the suction disc, two parts of an uncured stiff elastomer (Smooth-Sil 945, Smooth-On, Inc.) were mixed using a centrifugal mixer (ARE-310, Thinky). The uncured silicone was poured into the mold, degassed for 5 min, and cured at room temperature for 24 h. We added a nylon-sintered 3D printed (Fuse 1, Formlabs) threaded sleeve onto each disc stem with silicone adhesive (Sil-Poxy, Smooth-On Inc.) to interface with the robot arm for mechanical testing.

Fabrication of disc structures using thermoforming

Given that the suction discs were a non-planar geometry to which we were adding surface features, we used a combination of thermoforming and molding to incorporate the patterns. The patterns were designed using a graphic design software (CorelDRAW, Corel Co.) and rastered into a sheet (thickness, 1.5 mm) of polyethylene terephthalate glycol (PETG) via laser engraving (Universal Laser Systems, Inc.). The pattern was release-cut from the sheet of PETG and fixed with the rastered face up in a vacuum forming machine (85756, Micro-Mark, Co.). For the thermoforming process, we fabricated a rigid mold matching the internal suction chamber of the suction discs. The rastered PETG was uniformly heated using an overhead heater to 130°C for 40 s, and subsequently formed to the rigid mold below using a vacuum. The PETG was allowed to cool and released from the mold, providing a negative mold for the design (Fig. 6a,b).

The thermoformed PETG pattern was used to "stamp" the pad-like structures/channels into the disc by casting an additional soft silicone layer between the existing disc and the PETG sheet. A suction disc was placed in a rigid stand with the suction chamber facing up (Fig. 6c). A soft, two-part uncured silicone elastomer (Ecoflex 00-30, Smooth-On, Inc.) was combined with a silicone pigment (SilcPig, Smooth-On, Inc.) and prepared using a centrifugal mixer. The soft elastomer was then degassed for 2 min in a vacuum chamber.

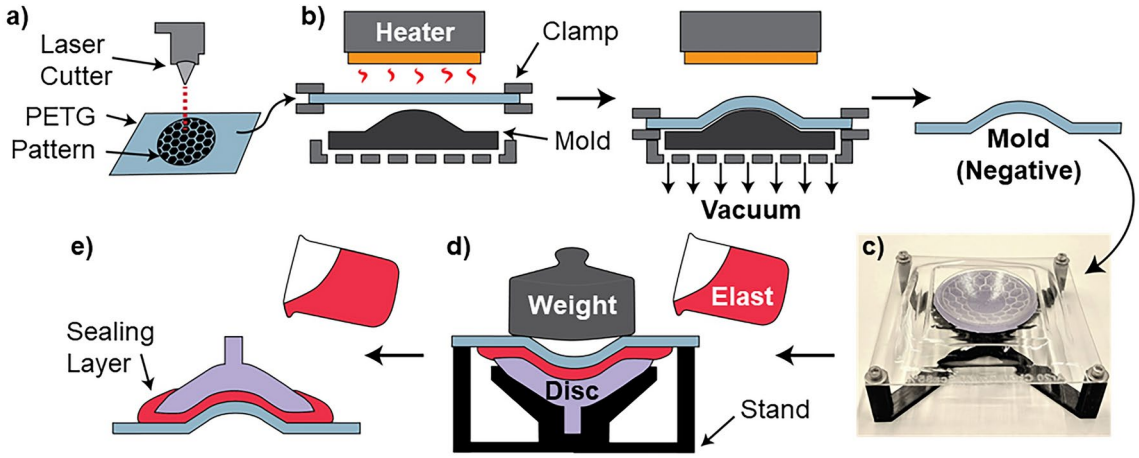

Figure 6. Fabrication process to produce desired surface patterning. (**a**) The pattern was rastered onto PETG using a laser microengraving machine. (**b**) A thermoformer heated the rastered PETG sheet, which then transferred onto the mold below, thereby forming to the desired shape when a vacuum was applied. Once cooled, the mold pattern was released. (**c**) An image of a thermoformed mold and suction disc (purple) in a stamping setup. Cup diameter was 60 mm. (**d**) Schematic of the elastomeric stamping process. Uncured elastomer was added to the chamber of a suction disc (supported by a stand). The thermoformed mold was fixed to the top and loaded with a weight. (**e**) A final sealing layer of uncured elastomer was applied to the back of the disc.

The uncured silicone was deposited on the face-up chamber of the suction disc, and to cavities in the mold of the negative design that was generated via thermoforming. Both components were degassed in a vacuum chamber for 3 min to remove air pockets that may have formed during the initial pour. The mold of the negative was inverted and stamped onto the suction chamber, secured at four corners by fasteners and loaded in the center by a 500 g weight to ensure an even distribution of silicone along the patterned mold (Fig. 6d). The height of the four corners of the stand were calculated to provide a 2 mm offset from the thermoformed mold to the surface of the suction disc, resulting in a soft layer that was 5 mm in thickness. The molded silicone was allowed to cure for 8 hr at room temperature.

Once the stamped silicone cured, the suction disc was removed from the stand and a sealing layer of elastomer (Ecoflex 00-30, Smooth-On, Inc.) was added along the interface of the stiff suction disc and the elastomeric layer to prevent delamination (Fig. 6e). The silicone was then trimmed after the final cure to remove flashing and regain the desired circular outline. As single cup was produced for each design.

Measuring mold dimensions

We characterized the resulting dimensions and surface finish of the laser-rastered patterned molds using 3D optical microscopy (Olympus Lext OLS4000). The surfaces of the molds were imaged in 3D using the focus-stacking functionality, which yielded the measurements for the pad areas and channel cross-sectional areas (e.g., width, depth).

Mechanical testing using a robotic arm

We measured the resistance to shear motion of the suction disc variants when adhered to a submerged surface using a robotic arm (UR5e, Universal Robots, Co.). An adapter at the end effector of the arm securely attached to the threaded sleeves of the suction discs. Using the force/torque sensor on the end effector of the robotic arm, we recorded the force resulting from a displacement in the x-direction, parallel to the surface, and z-direction, normal to the surface. An interchangeable plate, hosting the smooth substrate or the rough substrate, was mounted in the water tank, submerged in $\approx$1 cm of water (Fig. 5d,e).

Using a custom software and user interface, we programmed paths for the robotic arm to follow, per the trial type. Upon initialization of a trial while the disc was submerged but not yet contacting the target surface, the force sensor of the robotic arm was balanced. The robotic arm then translated in the $-z$-direction (downward), pushing the suction disc into the experimental surface and thereby preloading the disc. Upon reaching 10 N to fully compress the disc against the surface, the robotic arm would either translate in the $+z$-direction (upward) to the desired preload value (1–9 N) or maintain the full preload (10 N). By translating in the $+z$-direction, the preload was reduced, a vacuum chamber was formed, and suction was initialized. The initial compression of 10 N was used across all trials. After preloading, the robotic arm translated in the x-direction for 10 mm at a rate of 0.5 mm s^{-1}. Each trial was run in triplicate and post-processed in MATLAB. Shear stress (σ_{shear}, kPa) was quantified as the peak force (N) experienced while subjected to a shear disturbance with respect to the surface area of the undeformed suction disc (mm^2).

Data availability

All data generated or analysed during this study are included in this published article (and its Supplementary Information files).

Received: 20 August 2024; Accepted: 3 December 2024
Published online: 06 January 2025

References

1. Ditsche, P. & Summers, A. P. Aquatic versus terrestrial attachment: Water makes a difference. *Beilstein J. Nanotechnol.* **5**, 2424–2439 (2014).
2. Li, M. S., Melville, D., Chung, E. & Stuart, H. S. Milliscale features increase friction of soft skin in lubricated contact. *IEEE Robot. Autom. Lett.* **5**, 4781–4787 (2020).
3. Chen, Y. et al. Bioinspired multiscale wet adhesive surfaces: Structures and controlled adhesion. *Adv. Func. Mater.* **30**, 1905287 (2020).
4. Shorter, K. A., Murray, M. M., Johnson, M., Moore, M. & Howle, L. E. Drag of suction cup tags on swimming animals: Modeling and measurement. *Mar. Mamm. Sci.* **30**, 726–746 (2014).
5. Meynecke, J. & Liebsch, N. Asset tracking whales-first deployment of a custom-made gps/gsm suction cup tag on migrating humpback whales. *J. Mar. Sci. Eng.* **9**, 597 (2021).
6. Stuart, H. S. et al. Suction helps in a pinch: Improving underwater manipulation with gentle suction flow. In *IEEE/RSJ International Conference on Intelligent Robots and Systems* 2279–2284 (2015).
7. Sandoval, J. A., Xu, T., Adibnazari, I., Deheyn, D. D. & Tolley, M. T. Combining suction and friction to stabilize a soft gripper to shear and normal forces, for manipulation of soft objects in wet environments. *IEEE Robot. Autom. Lett.* **7**, 4134–4141 (2022).
8. Delroisse, J., Kang, V., Gouveneaux, A., Santos, R. & Flammang, P. *Convergent Evolution: Animal Form and Function*, 523–557 (Springer International Publishing, 2023).
9. Bagheri, H. et al. New insights on the control and function of octopus suckers. *Adv. Intell. Syst.* **2**, 1900154 (2020).
10. Tramacere, F. et al. The morphology and adhesion mechanism of octopus vulgaris suckers. *PLoS ONE* **8**, 65074 (2013).
11. Tramacere, F., Kovalev, A., Kleinteich, T., Gorb, S. N. & Mazzolai, B. Structure and mechanical properties of octopus vulgaris suckers. *J. R. Soc. Interface* **11**, 20130816 (2014).
12. Mazzolai, B. et al. Octopus-inspired soft arm with suction cups for enhanced grasping tasks in confined environments. *Adv. Intell. Syst.* **1**, 1900041 (2019).
13. Xie, Z. et al. Octopus arm-inspired tapered soft actuators with suckers for improved grasping. *Soft Rob.* **7**, 639–648 (2020).
14. Sareh, S. et al. Anchoring like octopus: Biologically inspired soft artificial sucker. *J. R. Soc. Interface* **14**, 20170395 (2017).
15. Tramacere, F., Appel, E., Mazzolai, B. & Gorb, S. N. Hairy suckers: The surface microstructure and its possible functional significance in the Octopus vulgaris sucker. *Beilstein J. Nanotechnol.* **5**, 561–565 (2014).
16. Zou, J., Wang, J. & Ji, C. The adhesive system and anisotropic shear force of guizhou gastromyzontidae. *Sci. Rep.* **6**, 37221 (2016).
17. Krings, W., Konn-Vetterlein, D., Hausdorf, B. & Gorb, S. N. Holding in the stream: convergent evolution of suckermouth structures in loricariidae (siluriformes). *Front. Zool.* **20** (2023).
18. Ditsche, P., Wainwright, D. K. & Summers, A. P. Attachment to challenging substrates-fouling, roughness and limits of adhesion in the northern clingfish (Gobiesox maeandricus. *J. Exp. Biol.* **217**, 2548–2554 (2014).
19. Ditsche, P. & Summers, A. Learning from northern clingfish (Gobiesox maeandricus): Bioinspired suction cups attach to rough surfaces. *Philos. Trans. R. Soc. B* **374**, 20190204 (2019).
20. Culler, M., Ledford, K. A. & Nadler, J. H. The role of topology and tissue mechanics in remora attachment. *MRS Online Proc. Libr.* **1648**, mrsf13-1648 (2014).
21. Kenaley, C. P., Stote, A., Ludt, W. B. & Chakrabarty, P. Comparative functional and phylogenomic analyses of host association in the remoras (echeneidae), a family of hitchhiking fishes. *Integr. Organ. Biol.* **1**, 007 (2019).
22. Gamel, K. M., Garner, A. M. & Flammang, B. E. Bioinspired remora adhesive disc offers insight into evolution. *Bioinspiration Biomimetics* **14**, 056014 (2019).
23. Cohen, K. E. et al. Sucker with a fat lip: The soft tissues underlying the viscoelastic grip of remora adhesion. *J. Anat.* **237**, 643–654 (2020).
24. Chuang, Y.-C., Chang, H.-K., Liu, G.-L. & Chen, P.-Y. Climbing upstream: Multi-scale structural characterization and underwater adheison of the pulin river loach (sinogastromyzon puliensis). *J. Mech. Behav. Biomed. Mater.* **73**, 76–85 (2017).
25. Briggs, J. C. *A monograph of the clingfishes (order Xenopterygii)*. Natural History Museum of Stanford University (1955).
26. Huie, J. M., Wainwright, D. K., Summers, A. P. & Cohen, K. E. Sticky, stickier and stickiest-a comparison of adhesive performance in clingfish, lumpsuckers and snailfish. *J. Exp. Biol.* **225**, jeb244821 (2022).
27. Wang, Y. et al. A biorobotic adhesive disc for underwater hitchhiking inspired by the remora suckerfish. *Sci. Robot.* **2**, eaan8072 (2017).
28. Sandoval, J. A., Jadhav, S., Quan, H., Deheyn, D. D. & Tolley, M. T. Reversible adhesion to rough surfaces both in and out of water, inspired by the clingfish suction disc. *Bioinspiration Biomimetics* **14**, 066016 (2019).
29. Wang, S. et al. Detachment of the remora suckerfish disc: kinematics and a bio-inspired robotic model. *Bioinspiration Biomimetics* **15**, 056018 (2020).
30. Huie, J. M. & Summers, A. P. The effects of soft and rough substrates on suction-based adhesion. *J. Exp. Biol.* **225**, jeb243773 (2022).
31. Wainwright, D. K., Kleinteich, T., Kleinteich, A., Gorb, S. N. & Summers, A. P. Stick tight: suction adhesion on irregular surface in the northern clingfish. *Biol. Let.* **9**, 20130234 (2013).
32. Thomas, J., Gorb, S. N. &Büscher, T. H. Influence of surface free energy of the substrate and flooded water on the attachment performance of stick insects (phasmatodea) with different adhesive surface microstructures. *J. Exp. Biol.* **226**, 244295 (2023).
33. Barnes, W. J. P., Baum, M., Peisker, H. & Gorb, S. N. Comparative cryo-sem and afm studies of hylid and rhacophorid tree frog toe pads. *J. Morphol.* **274**, 1384–1396 (2013).
34. Gong, L., Yu, H., Wu, X. & Wang, X. Wet-adhesion properties of microstructured surfaces inspired by newt footpads. *Smart Mater. Struct.* **27**, 114001 (2018).
35. Sandoval, J. A. et al. Toward bioinspired wet adhesives: Lessons from assessing surface structures of the suction disc of intertidal clingfish. *ACS Appl. Mater. Interfaces.* **12**, 45460–45475 (2020).
36. Hernandez, A. M., Sandoval, J. A., Yuen, M. C. & Wood, R. J. Stickiness in shear: stiffness, shape, and sealing in bioinspired suction cups affect shear performance on diverse surfaces. *Bioinspiration Biomimetics* **19**, 036008 (2024).
37. Persson, B.N.J. Wet adhesion with application to tree frog adhesive toe pads and tires. *J. Phys.: Condens. Matter* **19**, 3761104 (2007).
38. Endlein, T. et al. Sticking under wet conditions: The remarkable attachment abilities of the torrent frog. *Staurois guttatus. PLoS One* **8**, e73810 (2013).
39. Endlein, T. & Barnes, W. J. P. *Wet adhesion in tree and torrent frogs*. Encyclopedia of Nanotechnology (Springer, 2015).
40. Gordon, M. S., Fischer, S. & Tarifeño, E. Aspects of the physiology of terrestrial life in amphibious fishes. ii. the chilean clingfish, sicyases sanguineus. *J. Exp. Biol.* **53**, 559–572 (1970).

41. Fujiwara, K., Motomura, H., Summers, A. P. & Conway, K. W. A new generic name for the "lepadichthys" lineatus complex with a rediagnosis of discotrema, a senior synonym of unguitrema, and comments on their phylogenetic relationships (gobiesocidae: Diademichthyinae). *Vert. Zool.* **74**, 279–301 (2024).
42. Briggs, J. C. A new genus and species of clingfish from the western pacific. *Copeia* **1976**, 339–341 (1976).
43. Persson, B.N.J., Tartaglino, U., Albohr, O. & Tosatti, E. Rubber friction on wet and dry road surfaces: The sealing effect. *Phys. Rev. B Condens. Matt. Mater. Phys.* **71**, 035428 (2005).
44. Kamperman, M., Kroner, E., del Campo, A., McMeeking, R. M. & Arzt, E. Functional adhesive surfaces with "gecko" effect: The concept of contact splitting. *Adv. Eng. Mater.* **12**, 335–348 (2010).
45. Arzt, E., Gorb, S. & Spolenak, R. From micro to nano contacts in biological attachment devices. *PNAS* **100**, 10603–10606 (2003).
46. Peressadko, A. & Gorb, S. N. When less is more: Experimental evidence for tenacity enhancement by division of contact area. *J. Adhes.* **80**, 247–261 (2004).

Acknowledgements

We thank Alexander B. Rotheli for his preliminary work that helped us determine our disc materials and develop our thermoforming technique. We would also like to thank Dr. Clark Teeple who was essential in developing the robotic platform used for shear force data collection. We thank the many members of Project CETI for their support during this study. We thank Dr. Dimitri Deheyn from Scripps Institution of Oceanography for the use of microscopy facilities to image the suction discs of biological specimens. This study was funded by Project CETI via grants from Dalio Philanthropies and Ocean X; Sea Grape Foundation; Rosamund Zander/Hansjorg Wyss, Chris Anderson/Jacqueline Novogratz through The Audacious Project: a collaborative funding initiative housed at TED.

Author contributions

A.M.H., J.A.S and R.J.W conceived the study, A.M.H., J.A.S and M.C.Y designed the experiments, J.A.S. conducted the experiments, A.M.H. and J.A.S analyzed the results. A.M.H and M.C.Y. wrote the initial draft of the manuscript. All authors reviewed the manuscript.

Declarations

Competing Interests

Author Robert J. Wood holds stock in Fleet Robotics, Inc., a marine robotics company focused on robotic anti-biofouling.

Additional information

Supplementary Information The online version contains supplementary material available at https://doi.org/10.1038/s41598-024-82221-0.

Correspondence and requests for materials should be addressed to A.M.H.